

Design for moment redistribution in FRP plated RC beams

Deric John Oehlers*, Matthew Haskett^a and Mohamed Ali M.S.^b

*School of Civil, Environmental and Mining Engineering, University of Adelaide,
South Australia 5005, Australia*

(Received October 14, 2009, Accepted February 22, 2011)

Abstract. Assessing the ductility of reinforced concrete sections and members has been a complex and intractable problem for many years. Given the complexity in estimating ductility, members are often designed specifically for strength whilst ductility is provided implicitly through the use of ductile steel reinforcing bars and by ensuring that concrete crushing provides the ultimate limit state. As such, the empirical hinge length and neutral axis depth approaches have been sufficient to estimate ductility and moment redistribution within the bounds of the test regimes from which they were derived. However, being empirical, these methods do not have a sound structural mechanics background and consequently have severe limitations when brittle materials are used and when concrete crushing may not occur. Structural mechanics based approaches to estimating rotational capacities and rotation requirements for given amounts of moment redistribution have shown that FRP plated reinforced concrete (RC) sections can have significant moment redistribution capacities. In this paper, the concept of moment redistribution in beams is explained and it is shown specifically how an existing RC member can be retrofitted with FRP plates for both strength and ductility requirements. Furthermore, it is also shown how ductility through moment redistribution can be used to maximise the increase in strength of a member. The concept of primary and secondary hinges is also introduced and it is shown how the response of the non-hinge region influences the redistribution capacity of the primary hinges, and that for maximum moment redistribution to occur the non-hinge region needs to remain elastic.

Keywords: reinforced concrete; moment redistribution; member ductility; fibre reinforced polymer; FRP; plated structure; hinge; member strength

1. Introduction

The ductility, and consequently the ability to redistribute moment, of reinforced concrete (RC) members is a very important structural design property as it governs not only the monotonic strength of a reinforced concrete structure but also its ability to resist dynamic loads such as blast and seismic loads (Yeh and Chang 2007, Hashemi *et al.* 2008a, Sharma *et al.* 2010, Howser *et al.* 2010). Ductility and moment redistribution have historically been very difficult concepts to estimate in reinforced concrete members. Various parameters have been recognised to influence ductility and

*Corresponding author, Professor, E-mail: doehlers@civeng.adelaide.edu.au

^aPh.D. Student

^bSenior Lecturer

moment redistribution, including section depth, bar diameter, and span length (Panagiotakos and Fardis 2001). These parameters are used to quantify a hinge length (L_{hinge}) which is subsequently used to determine the rotation, where rotation is simply the hinge length multiplied by the curvature at failure (χ_{ult}).

The curvature at failure is given by $\chi_{ult} = \varepsilon_c / (k_u d)$, where $k_u d$ is the depth of the neutral axis and ε_c is the strain at concrete failure and which is assumed to be constant. Expressing the hinge length in terms of the section depth, the rotation at failure is inversely proportional to the neutral axis parameter k_u . Hence, sections that are under-reinforced with small neutral axis parameters have greater rotation capacity and ductility at failure. The simplicity of this approach in estimating ductility has ensured that most codes worldwide prescribe moment redistribution in terms of the neutral axis parameter k_u .

While the k_u approach is both widely accepted and simple to apply, it is severely limited by the accuracy of the empirically derived hinge length expressions and the requirement that concrete crushing is the singular mode of failure. In plated beams (Hashemi *et al.* 2008b, Mahini and Ronagh 2009), it is much more common for debonding to occur well before the concrete crushes (Oehlers *et al.* 2004, Duthinh and Starnes 2004, Bencardino *et al.* 2002, Benlloch *et al.* 2002). As such, the rotational capacity of the 'hinge' in plated beams is no longer proportional to the factor ε_c / k_u , and therefore the approach can not be used in its current form for plated structures where plate debonding occurs prior to crushing. The k_u approach to estimating ductility also assumes a linear strain profile over the section depth, assuming full interaction between the reinforcement and the surrounding concrete. However, full interaction does not occur in reinforced concrete members adjacent to cracks, rendering this assumption an approximation. Hence, a partial interaction structural mechanics based approach is required to estimate ductility to model the behaviour of any reinforced concrete member for any failure mode.

This structural mechanics based approach for moment redistribution is also required because at present existing design guidelines (Concrete Society 2000, International Federation for Structural Concrete 2001) tend to ignore any moment redistribution capacities even though experimentally (Oehlers and Seracino 2004, Liu *et al.* 2006, Mukhopadhyaya *et al.* 1998, El-Refaie *et al.* 2003) substantial moment redistribution has been shown to occur in FRP plated beams.

In this paper: the concepts of moment redistribution are explained in full, a structural mechanics moment-rotation moment redistribution approach is outlined; the importance of the member ductility of the non-hinge region on moment redistribution is explained; and plated reinforced concrete members are specifically designed for moment redistribution. Through way of an example, a plated section is optimally designed for moment redistribution.

2. Moment redistribution

To illustrate moment redistribution, consider the built-in beam in Fig. 1(a) of span L and a constant flexural rigidity EI that is subjected to a uniformly distributed load w that induces moments at the supports M . From structural mechanics, it can be shown that whilst the beam remains elastic then the hogging moment M_h is $2/3^{\text{rd}}$ the static moment M_{st} and the sagging moment M_s is $1/3^{\text{rd}}$ M_{st} as shown in Fig. 1(b). Any change in the distribution as shown in Fig. 1(b) will require the formation of a hinge.

If the moment at the supports M_h is less than $2/3^{\text{rd}}$ M_{st} , then this means that a hinge has formed at

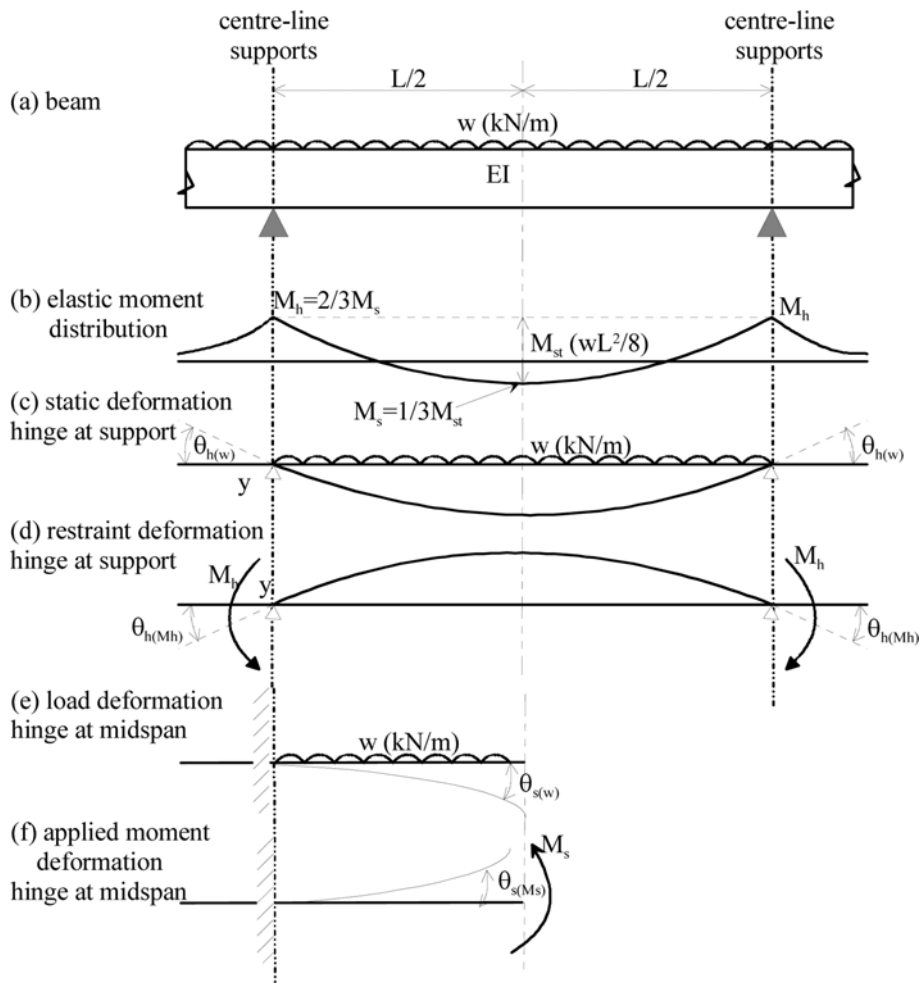


Fig. 1 Moment redistribution in a built in beam

the supports which has to rotate to allow the static moment to be achieved. In this case, moment is being redistributed from the hogging region to the sagging region. The amount of rotation required at the hinge θ_h is simply the difference between the rotation due to the static load $\theta_{h(w)}$ as shown in Fig. 1(c) and the rotation due to the support moment $\theta_{h(M_h)}$ in Fig. 1(d) which can be determined from elementary structural mechanics. If the moment at the supports is greater than $2/3^{\text{rd}}$ M_{st} , then a hinge needs to form at mid-span in which case the deformations in Figs. 1(e) and (f) apply so that the hinge at mid-span has to rotate $\theta_{s(M_s)} - \theta_{s(w)}$. In this case, the moment is being redistributed from the sagging region to the hogging region. It can be seen that the ability of the member to redistribute moment depends on the hinge rotation capacity.

Let us define the moment redistribution factor K_{MR} as the moment redistributed as a proportion of the elastic moment should redistribution not have occurred. For the case of the built-in beam in Fig. 1 with a uniformly distributed load w where the elastic hogging moment is $2/3^{\text{rd}}$ M_{st} and a hinge forms at the supports then

$$K_{MR(udl:h \rightarrow s)} = \frac{2/3 M_{st} - M_h}{2/3 M_{st}} \quad (1)$$

where $100K_{MR}$ is the well known percentage moment redistribution in national standards and where the subscript *udl* refers to uniformly distributed loads and *hs* to moment redistribution from the hogging region to the sagging region. Then allowing for the rotations in Figs. 1(c) and (d) (Haskett *et al.* 2010, Oehlers *et al.* 2010), the moment redistribution for a hinge forming at the support is given by

$$K_{MR(udl)} = \frac{2EI\theta_{cap}}{2EI\theta_{cap} + M_{cap}L} \quad (2)$$

Eq. (2) also applies for the case of a hinge forming at mid-span, that is allowing for the rotations in Figs. 1(e) and (f) (Haskett *et al.* 2010).

The moment (M_{cap}) and rotation (θ_{cap}) for any failure mechanism can be determined using a rigid body rotation approach (Oehlers *et al.* 2010, Haskett *et al.* 2009), that uses both partial interaction and shear friction theory. Hence, knowing these parameters and the flexural rigidity of the member and span length, the moment redistribution capacity of a section can be determined, independent of any hinge length but which allows for any mode of failure. It can be seen in Eq. (2) that the moment redistribution capacity depends on the flexural rigidity EI . However the flexural rigidity occurs in both the numerator and denominator so that the moment redistribution capacity is not that sensitive to EI . Consequently, the flexural rigidity of the cracked section (EI_{cr}) can be used since cracking would be expected, and this would provide a conservative estimate of the moment redistribution capacity. Although not the subject of the research in this paper, an equivalent EI between the cracked and uncracked flexural rigidity as used in determining deflections in national standards may also be appropriate.

3. Moment redistribution capacity of reinforced concrete members

3.1 Redistribution from support

Consider a continuous beam subjected to a uniformly distributed load as shown in Fig. 2 where the hinges first form at the supports as shown such that moment is redistributed from the hogging (-'ve) region to the sagging (+'ve) region. This section can be unplated or plated with a hogging moment capacity of M_{hog} (i.e., M_{cap} for the hogging hinge) and a sagging moment capacity of M_{sag} , such that the distribution of moment at failure is shown as curve A in Fig. 2. The static moment capacity, M_{static} , is simply the sum of the hogging (-'ve) and sagging (+'ve) moment capacities, as shown in Fig. 2 as the difference in peak moments in curve A. Under elastic conditions with no moment redistribution, the hogging moment M_{hog} is twice the sagging moment M_{sag} and the static moment is $3M_{hog}/2$. Hence if M_{hog} is less than $2M_{sag}$, then moment redistribution is required from the supports and the hinge needs to rotate which depends on the rotational capacity of the hinge, θ_{cap} (Haskett *et al.* 2010). It is, therefore, a question of determining whether the support hinge has sufficient rotational capacity to allow for this moment redistribution. The simplest solution is to determine what is the maximum sagging moment, $(M_{sag})_{redist}$ in Fig. 2, that the support hinge can accommodate so that if the sagging capacity, M_{sag} , is less than $(M_{sag})_{redist}$ then the hinge can

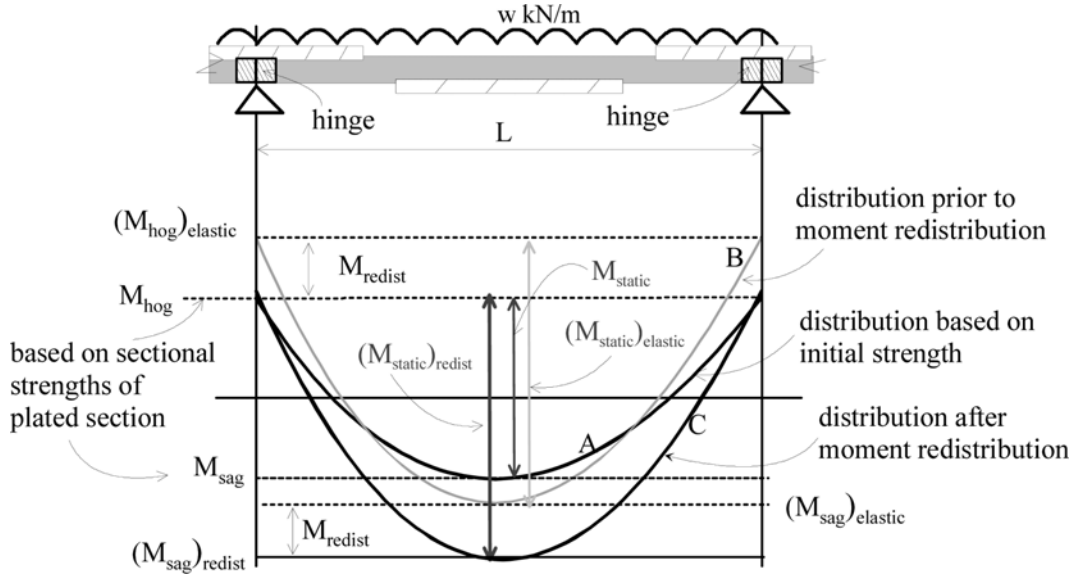


Fig. 2 Moment redistribution- from support

accommodate the rotation. Furthermore, $(M_{sag})_{redist} - M_{sag}$ is the maximum increase in the sagging strength that can be accomplished by FRP retrofitting. It is also worth noting that this increase in strength, $(M_{sag})_{redist} - M_{sag}$, occurs in a region where hinge rotation is not required so that brittle forms of retrofitting such as the use of externally bonded (EB) plates can be applied in this region. In contrast, the hinge region at the supports requires rotational capacity such that ductile forms of plating such as near surface mounted (NSM) plates may be appropriate.

From the hinge moment-rotation analysis mentioned in Section 2, the moment M_{cap} and rotation θ_{cap} at failure of the hinge can be determined. In this example of a continuous member subjected to a uniformly distributed load, the moment redistribution capacity of the hinge K_{MR} is given by Eq. (2). Then by the definition of K_{MR} , which is the redistributed moment M_{redist} in Fig. 2 as a proportion of the *elastic moment* $(M_{hog})_{elastic}$, i.e., $M_{redist}/(M_{hog})_{elastic}$, the maximum *elastic moment* at the support, $(M_{hog})_{elastic}$, is given by

$$(M_{hog})_{elastic} = \frac{M_{hog}}{(1 - K_{MR})} \quad (3)$$

where M_{hog} is the hogging moment capacity, and referred to as M_{cap} in Section 2, obtained from the rigid body rotation (RBR) model. As shown in Fig. 2, the *elastic moment* at midspan (i.e., the sagging region) is half that at the support and substituting Eq. (3) gives

$$(M_{sag})_{elastic} = \frac{(M_{hog})_{elastic}}{2} = \frac{M_{hog}}{2(1 - K_{MR})} \quad (4)$$

Hence the *elastic static moment*, shown in Fig. 2, which is the sum of Eqs. (3) and (4) is

$$(M_{static})_{elastic} = \frac{3M_{hog}}{2(1 - K_{MR})} \quad (5)$$

where the elastic distribution of moment is given by curve B in Fig. 2.

Since the maximum flexural capacity from the RBR analysis of the hogging region is M_{hog} , then the amount of moment redistributed from the hogging region to the sagging region is the difference between $(M_{hog})_{elastic}$ and M_{hog} , that is

$$M_{redist} = \frac{M_{hog} K_{MR}}{(1 - K_{MR})} \tag{6}$$

Redistributing the moment by definition moves the elastic distribution B to the redistributed moment variation of curve C. Consequently, the maximum sagging moment is given by

$$(M_{sag})_{redist} = \frac{M_{hog}(1 + 2K_{MR})}{2(1 - K_{MR})} \tag{7}$$

Thus, the maximum moment the sagging region can attain is limited by the redistribution capacity of the hogging region. Thus plating can be used to increase the strength of the sagging region up to $(M_{sag})_{redist}$. Any increase in strength beyond $(M_{sag})_{redist}$ is ineffective because rotational failure of the hogging hinge region occurs when it tries to redistribute moment in excess of its redistribution capacity, K_{MR} .

Consequently moment redistribution increases the static moment capacity, and hence the applied load capacity, w , by $(M_{static})_{elastic}/(3M_{hog}/2)$, that is by a factor of

$$\frac{1}{(1 - K_{MR(h \rightarrow s)})} \tag{8}$$

3.2 Redistribution from midspan

A similar approach can also be used when moment redistribution is occurring from midspan (sagging +ve region) to the support (hogging -ve region), as shown in Fig. 3.

The maximum *elastic moment* at midspan is given by

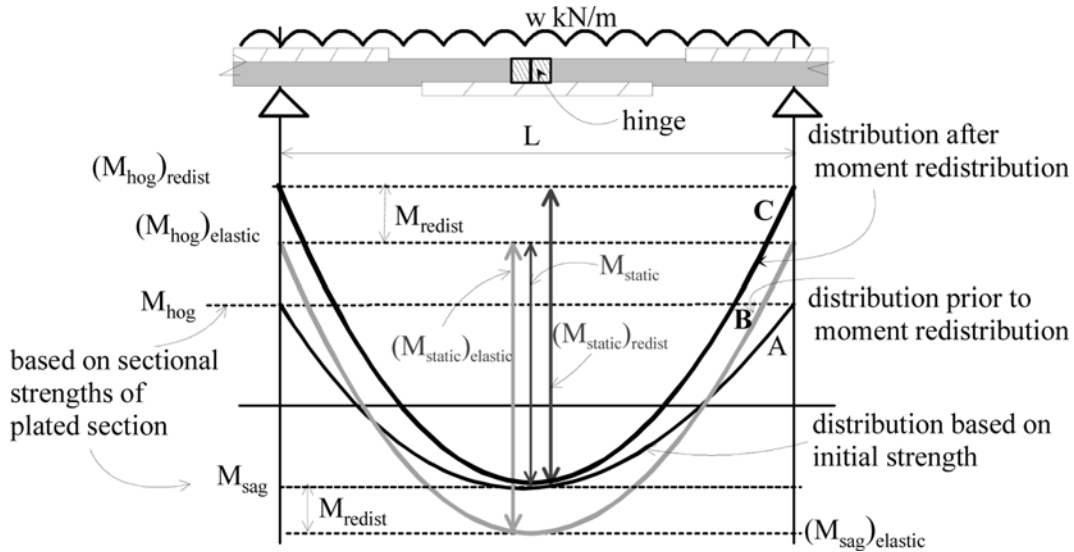


Fig. 3 Moment redistribution- from midspan

$$(M_{sag})_{elastic} = \frac{M_{sag}}{(1 - K_{MR})} \quad (9)$$

where M_{sag} is the moment capacity, referred to as M_{cap} in Section 2, of the sagging region from the RBR model. The *elastic moment* at the supports (hogging region) is twice the midspan moment

$$(M_{hog})_{elastic} = 2(M_{sag})_{elastic} = \frac{2M_{sag}}{(1 - K_{MR})} \quad (10)$$

The *elastic static moment* is

$$(M_{static})_{elastic} = \frac{3M_{sag}}{(1 - K_{MR})} \quad (11)$$

Since the maximum flexural capacity of the sagging region is M_{sag} , then the amount of moment redistributed from the sagging region to the hogging region is the difference between $(M_{sag})_{elastic}$ and M_{sag} , that is

$$M_{redist} = \frac{M_{sag}K_{MR}}{(1 - K_{MR})} \quad (12)$$

The hogging moment after redistribution is therefore

$$(M_{hog})_{redist} = \frac{M_{sag}(2 + K_{MR})}{(1 - K_{MR})} \quad (13)$$

As before, moment redistribution increases the static moment capacity by a factor of

$$\frac{1}{(1 - K_{MR(s \rightarrow h)})} \quad (14)$$

The maximum moment the hogging region can attain is limited by the redistribution capacity of the sagging region. Thus plating can be used to increase the strength of the hogging region to $(M_{hog})_{redist}$. Any increase in strength beyond this is prevented by the limited rotational capacity of the sagging (+ve) region hinge. That is, plating the hogging region beyond $(M_{hog})_{redist}$ is ineffective because rotational failure of the sagging region occurs when it tries to redistribute moment in excess of its redistribution capacity, K_{MR} . In this scenario, brittle FRP plating techniques can be used in the hogging regions, whereas, ductile FRP plating techniques are required in the sagging region.

To complete the picture, the third option to increase the applied load, w , is to plate both the sagging and hogging regions such that the capacity of the hogging region remains at twice that of the sagging region, that is the moment distribution remains elastic so that rotation is not required and, hence, brittle forms of FRP plating could be used throughout. Provided the ratio of the hogging and sagging region moment capacities remains 2:1, then there is no need for moment redistribution since an elastic moment distribution is achieved. In this situation, plating is theoretically unlimited since the moment ratio remains at 2:1 and no rotational capacity is required since neither possible hinge location is required to redistribute moment. However this is a brittle design philosophy and consequently unsafe and should be avoided or used with an increased factor of safety. Ductility should always be considered in all designs and hence plated sections should always be provided with some degree of ductility to allow the member to accommodate, amongst other things, a load distribution other than what it was originally designed for.

Eq. (7) and shown in Fig. 2. The moment $(M_{sag})_{redist}$ is the maximum moment that can be attained at midspan corresponding to the hogging region redistributing its maximum capacity.

The non-hinge region, that is the region having the moment redistributed to it, in this example the sagging region, needs to remain elastic to prevent any rotation at midspan from occurring. If rotation occurs at midspan prior to $(M_{sag})_{redist}$ being achieved, then this rotation at midspan is also induced in the hogging hinge. That is, if a rotation of magnitude $(\theta_{sag})_{redist}$ is induced at midspan, then the actual total rotation at the hogging hinge is $\theta_{cap} + (\theta_{sag})_{redist}$. Since the rotation capacity of the hinge is θ_{cap} and the entire rotation capacity has been utilised to redistribute K_{MR} , then any additional hinge rotation induced by rotation at midspan will cause rotational failure within the hinge. However, if $(M_{sag})_{redist}$ is elastic, that is $(\theta_{sag})_{redist}$ is negligible, then the additional rotation induced in the hinge due to midspan rotation is also negligible, and therefore, rotational failure of the hinge will not occur. If $(M_{sag})_{redist}$ is not elastic, then $(\theta_{sag})_{redist}$ is not negligible and, hence, failure will occur within the hogging hinge.

For the sagging region to remain elastic, $(M_{sag})_{redist}$ must lie on O-D in Fig. 4. If $(M_{sag})_{redist}$ is less than M_{yield} , then the existing section can accommodate full moment redistribution. If $(M_{sag})_{redist}$ is greater than M_{yield} then the sagging region must be plated such that reinforcing bar yield occurs after $(M_{sag})_{redist}$. As an example, for $(M_{sag})_{redist} = M_I$, position I in Fig. 4 is suitable. In summary, the moment rotation capacity of Eq. 2 requires the non-hinge region to remain elastic. If this is not the case, then the hinge needs additional rotation capacity as follows.

3.3.2 Generic behaviour

Consider a generic moment-rotation relationship where there is an increase in flexural strength post yield due to the strain hardening behaviour of the steel reinforcement. An example is the moment-rotation response O-A-C in Fig. 4. Let us assume that the same hinge response O-A-C exists in both the sagging and hogging regions. For this case, an iterative approach to determine the redistribution capacity of the hinge is required.

As a first estimate in our analysis, let us assume that maximum moment redistribution can occur, and the moment and rotation of the hinge is C in Fig. 4. For M_{cap} and θ_{cap} , determine the redistribution capacity of the hinge K_{MR} from Eq. (2) to determine $(M_{sag})_{redist}$. As before, if $(M_{sag})_{redist}$ is less than M_{yield} then the rotation at midspan due to redistribution is minimal and as the sagging region remains elastic, full redistribution can occur. In this case no iteration is necessary to find the redistribution capacity of the hinge.

If $(M_{sag})_{redist}$ is greater than M_{yield} , then the sagging region can be plated such that reinforcing bar yield occurs after $(M_{sag})_{redist}$, shown as O-D in Fig. 4. Once again, in this case no iteration is necessary to find the redistribution capacity since the sagging region remains elastic and does not induce any additional rotation requirements within the hinge.

If $(M_{sag})_{redist}$ is greater than M_{yield} and less than M_{cap} , then the existing member does not need to be retrofitted to accommodate moment redistribution. However, full moment redistribution can not occur since the sagging region is on A-C in Fig. 4, and hence rotation is occurring at midspan whilst moment is being redistributed to it. Consequently, the hogging hinge has to rotate more than θ_{cap} to accommodate the additional rotation. The iterative approach to determining the peak amount of moment redistribution is as follows.

Guess a moment and rotation at the hogging hinge, with $M < M_{cap}$; for example H in Fig. 4. For M_H and θ_h determine K_{MR-H} . For K_{MR-H} determine $(M_{sag})_{redist}$ as before, and which we will refer to as M_S in this example. For M_S determine the corresponding rotation, θ_S . This rotation θ_S occurs at

midspan and is also induced at the support. Hence, the total rotation at the support (primary) hinge is $\theta_{total} = \theta_H + \theta_S$. If θ_{total} is greater than the rotation capacity of the section θ_{cap} , for example E in Fig. 4, then rotational failure will occur and the original guess of the rotation was too high and needs to be reduced. If θ_{total} is less than θ_{cap} , for example F in Fig. 4, then the full rotational capacity of the hinge is not being utilised and, therefore, the original guess of rotation is too low and further rotation and redistribution can be accommodated. If θ_{total} is equal to θ_{cap} , C in Fig. 4, then the assumed rotation θ_h was correct and the maximum amount of moment has been redistributed.

4. Moment redistribution mechanism

The moment redistribution mechanism is illustrated in Fig. 5 for a beam subjected to a uniformly distributed load w as in Fig. 5(a), where the moment at the support is M_1 and that at mid-span M_2 ,

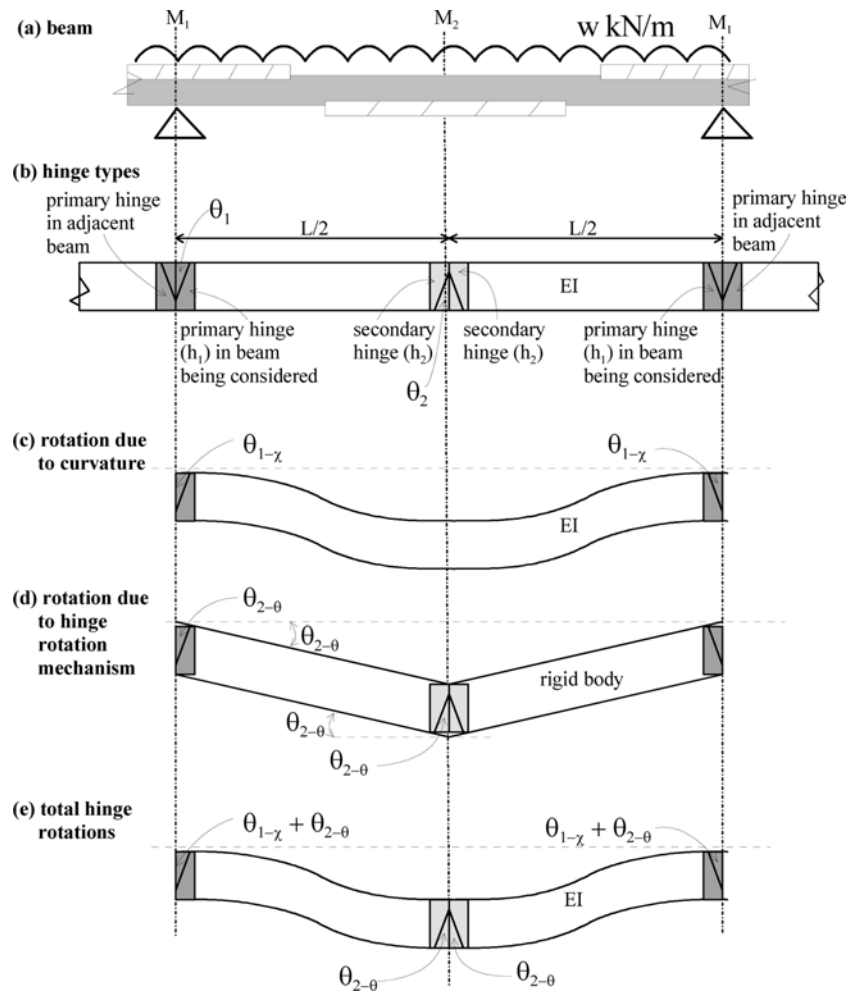


Fig. 5 Redistribution mechanism from hogging (-'ve) to sagging (+'ve) region

and where moment is being redistributed from the hogging region to the sagging region. In this section, the moment redistribution mechanism will be illustrated for this case of redistribution from the hogging region to the sagging region, although, it applies in principle for redistribution from the sagging region to the hogging region.

The moment redistribution Eq. (2) dealt with the conventional case where rotation occurred at the hogging hinge to accommodate the deformation between hinges due to curvature, χ , as shown in Fig. 5(c), and where the non hinge region remained elastic. It has been suggested in Sect. 2 that, to obtain a conservative estimate of the moment redistribution factor K_{MR} , the cracked flexural rigidity of the cracked section $(EI)_{cr}$ could be used in the analysis as this would over-estimate the rotation required. The rotation $\theta_{1-\chi}$ in Fig. 5(c) is, therefore, the hinge rotation required in Eq. (2) to develop a specific value of K_{MR} due to the variation in curvature along the beam between the hinges.

In reality, flexural cracks generally occur at the early stages of loading in the regions of maximum moment, M_1 and M_2 in Fig. 5(a), and as shown in Fig. 5(b) and which can rotate as shown in Fig. 6 where reinforcement yielding occurs at (M_y, θ_y) . However, it should be remembered that the ‘elastic rotation’ prior to yielding is a least one order of magnitude smaller than the ‘plastic rotation’ shown. Hence a better way of visualising the problem, and much closer to reality, is shown in Fig. 5(b) where hinges are present in both the hogging and sagging regions from the onset of loading; this allows for the flexural cracks at the position of maximum moments and consequently the flexural rigidity between hinges may be better represented by the flexural rigidity of the uncracked section as shown.

The hinge which sheds its moment to the other hinge will be referred to as the primary hinge as shown in Fig. 5(b), so that the hinge where moment is being shed to will be referred to as the secondary hinge. The rotation of the primary hinge is shown as θ_1 and that of the secondary hinge as θ_2 . It may also be worth noting that the hinge at mid-span is shown as two adjacent hinges as the analysis in Sect. 2 gives the rotation in each individual hinge.

The rotation $\theta_{1-\chi}$ of the primary hinge in Fig. 5(c) is the rotation for a given amount of moment redistribution that is required by the primary hinge to accommodate the curvature distribution along the beam. The rotation in Fig. 5(d) is the rigid body rotation induced by the secondary hinge mechanism, where its magnitude is a function of the amount of moment redistribution from the primary hinge, and the secondary hinge’s $M-\theta$ response. This rotation is independent of the curvature distribution and solely a function of the $M-\theta$ response of the secondary hinge. Hence if the secondary hinge rotates $\theta_{2-\theta}$ as shown, then the primary hinge has also to rotate the same value to maintain compatibility. Hence, the total hinge rotations are as in Fig. 5(e) where the primary hinge has to rotate

$$\theta_{1-total} = \theta_{1-\chi} + \theta_{2-\theta} \quad (15)$$

If the secondary hinge remains ‘elastic’ as shown in Fig. 6, then the rotation of the secondary hinge, $\theta_{2-\theta}^*$ is very small and can be ignored so that the rotation required at the primary hinge remains at $\theta_{1-\psi}$ as in Eq. (2) and in Eq. (15). If the secondary hinge yields and strain hardens then the rotation $\theta_{2-\theta}$ in Eq. (15) cannot be ignored.

5. Application of design for moment redistribution

The basics of moment redistribution have been explained in the previous section. An example is

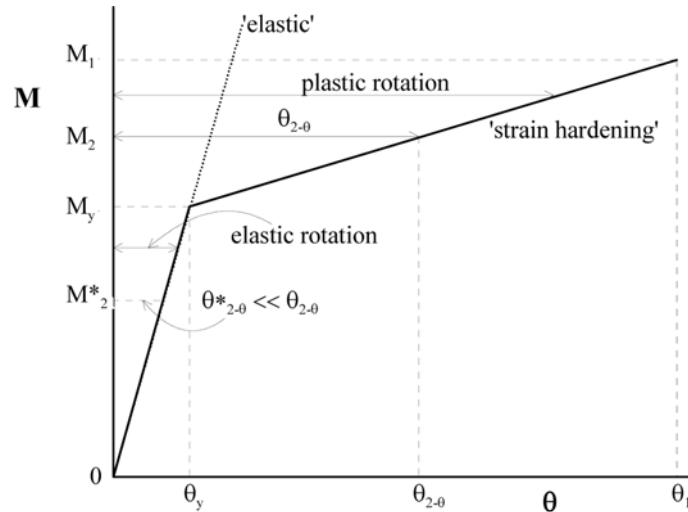


Fig. 6 Rigid body rotations

now provided to demonstrate the ability to now design for ductility in addition to flexural strength. Consider the RC section shown in Fig. 7, with its moment-rotation response from the RBR approach shown in Fig. 8, where the capacity at failure can be taken as 100 kNm at a rotation of 0.08 radians, and that at yield as 80 kNm with very minor rotation. This section is assumed to occur in both the hogging and sagging regions of the member.

5.1 Redistribution capacity of RC sections: both regions plastic

As the hogging and sagging moment capacities are 100 kNm, the theoretical maximum static moment, assuming unlimited rotational ductility, is 200 kNm. Allowing for rotational ductility, the

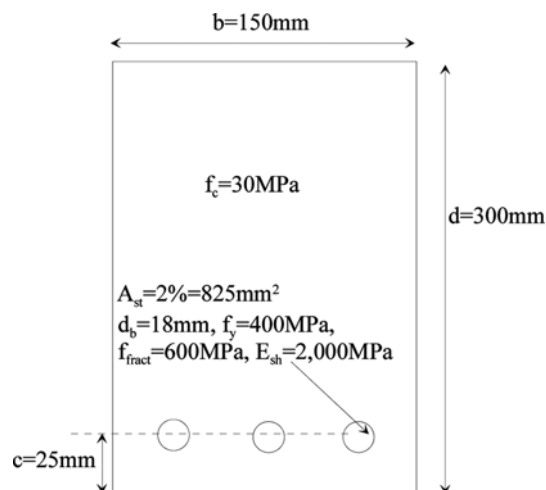


Fig. 7 300 mm deep RC section

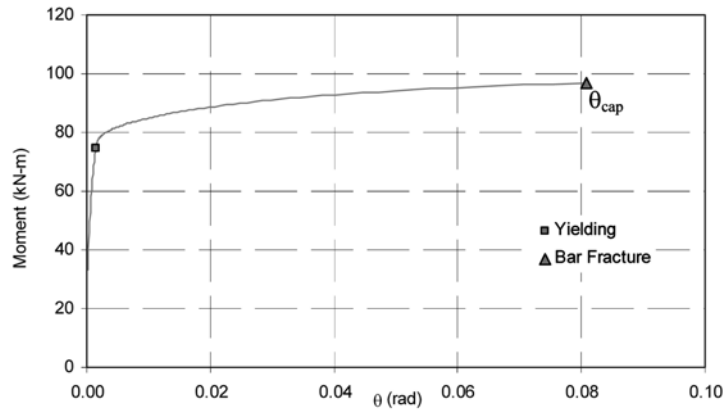


Fig. 8 Moment-rotation response of unplated RC section

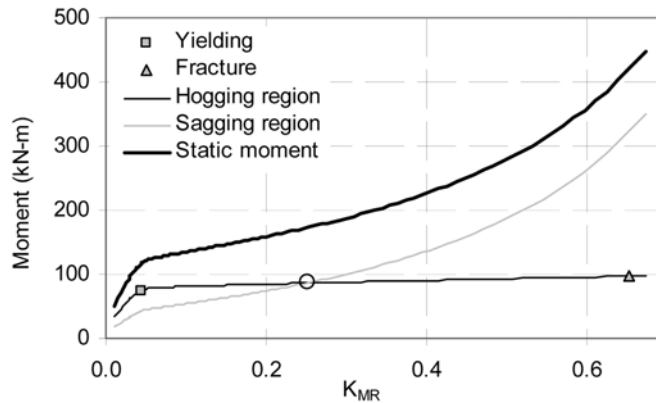


Fig. 9 Total static moment for given amounts of moment redistribution

iterative technique described in Section 3.3.2 can be used to determine the actual static moment capacity of the member, with both hogging and sagging regions having hinges with the same $M-\theta$ hinge response as in Fig. 8.

The $M-\theta$ response in Fig. 8 can be converted to a $M-K_{MR}$ response, shown as the faint black line in Fig. 9, and where bar yield and fracture are also shown. For the given amount of moment redistribution on the abscissa, the corresponding moment in the sagging region is also determined, and shown as the faint grey line in Fig. 9. The total static moment, that is the sum of the moments in the hogging and sagging regions, is shown as the bold black line.

In Fig. 9, it can be seen that under initial loading the moment distribution is virtually elastic, where the sagging moment is very close to half the hogging moment. It is worth noting that it is ‘virtually elastic’ because, as shown in Fig. 8, it is assumed that there is some miniscule rotation prior to yield, that is a crack is present at the start of loading which rotates as discussed previously. After the bars yield, the hogging primary hinge rotates and redistributes moment to the sagging secondary hinge. As the hogging hinge continues to rotate, the moment redistribution increases and at some point, in this example $K_{MR} = 0.25$ and shown as the black circle, the moment in the sagging hinge exceeds the moment in the hogging region. The redistribution continues until ultimately

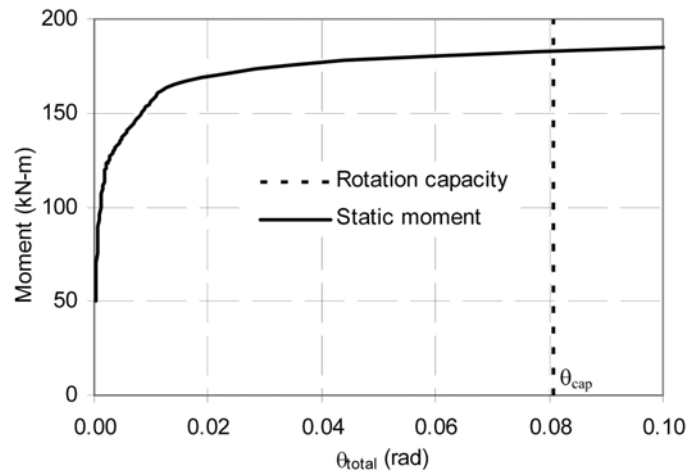


Fig. 10 Static moment and total hinge rotation

hogging hinge failure occurs when the hogging hinge has no rotational capacity remaining. In Fig. 9, the total static moment capacity of the member at failure is approximately 415 kNm, and this capacity can only be achieved if the sagging secondary hinge remains elastic, that is the sagging hinge has not yielded.

If the same section is used in both regions with the $M-\theta$ response shown in Fig. 8, the amount of redistribution required in the previous paragraph cannot occur and limits to moment redistribution due to additional rotation at the secondary hinge are introduced. As redistribution increases, the moment at midspan increases and hence so too does the rotation. Thus, the total rotation at the primary hinge is the rotation for a given amount of moment redistribution due to curvature and referred to as $\theta_{1-\chi}$ in Fig 5, plus any midspan rotation induced in the secondary hinge by moment redistribution, $\theta_{2-\theta}$ in Fig. 5. The total rotation at the hinge, θ_{total} , referred to as $\theta_{1-total}$ in Eq. (15) previously, and the static moment are graphed in Fig. 10, where a limit to the rotation is shown as the black dotted line at θ_{cap} .

It can be seen in Fig. 10 that at primary hinge failure the total static moment capacity is 183 kNm. From Fig. 9 for this static moment, the moment in the hogging hinge is 87 kNm, and the moment in the sagging hinge is 96 kNm. The rotation corresponding to these moments from Fig. 8 is $1.5E-2$ and $6.3E-2$ radians in the hogging and sagging hinges respectively. The total rotation θ_{total} in the hogging hinge is, therefore, the sum of these two rotation, $8E-2$ radians, which is the rotation capacity at bar fracture (θ_{cap}) in Fig. 8. In this example, the primary hinge redistributes 28% moment at failure, and where the limit on redistribution is caused by the sagging secondary hinge behaving plastically.

The relative contribution of each hinge in terms of moment and rotation for a given static moment are shown in Fig. 11. It can be seen that for small static moments the moment distribution is elastic, as the hogging moment shown as the black line is approximately $2/3$ the static moment, and the sagging moment is $1/3$ the static moment and shown as the grey line. As the static moment increases and the hogging hinge yields, increased redistribution to midspan occurs. Accordingly, due to the increased moment, the crack width at midspan increases and begins to rotate more. After yield of the hogging hinge, shown in Fig. 11 as a grey triangle, the hogging rotation increases and

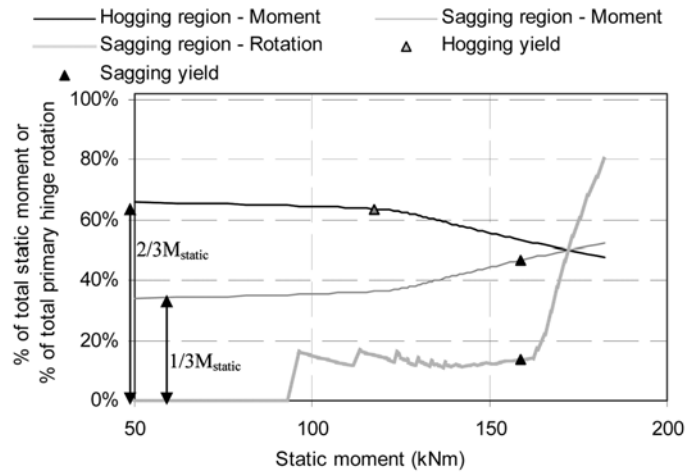


Fig. 11 Relative rotation and moment contributions for both regions for a given static moment

hence the redistribution to midspan increases. This is shown in Fig. 11 where the relative contribution of the hogging hinge to the total static moment reduces post yield and the contribution of the sagging hinge increases. Ultimately this increased moment at midspan causes the reinforcing bars at midspan to yield, shown as the black triangle in Fig. 11. The presence of yielding at midspan induces larger rotations at midspan and this rotation is also induced at the hogging hinge. Since the moment at failure is, in this example, greater at midspan (the secondary hinge) than at the primary hinge, the majority of the primary hinge rotation at failure is induced by the secondary hinge rotation. In this example, 80% of the total primary hinge rotation at failure is induced by the secondary hinge rotation. From Eq. (15), at failure $\theta_{2-\theta}$ is 80% of $\theta_{1-total}$, and $\theta_{1-\chi}$ is 20% of $\theta_{1-total}$.

Without performing a parametric study, it should be noted that for an RC member the relationship between the relative moments at midspan and at the support at failure are closely correlated to the strain hardening modulus and fracture strain of the reinforcing bars. The strain hardening modulus significantly influences the post yield stiffness of the $M-\theta$ response, shown as κ_1 in Fig. 4. For increasing strain hardening modulus (and constant bar fracture strain) κ_1 increases post yield, resulting in less moment redistribution capacity. In this situation, the amount of moment redistributed to the midspan region is reduced and hence the primary hinge contributes more to the total static moment capacity. The amount of rotation within the primary hinge induced by any secondary hinge rotation is also limited.

The total static moment capacity of the existing member (i.e., ignoring any plating considerations) is 183 kNm, corresponding to 28% moment redistribution. The predicted RBR redistribution and code moment redistribution allowances are compared in the following section. Plated RC sections are then analysed for moment redistribution, where it is assumed that the non-hinge region remains elastic; that is the secondary hinge region remains elastic.

5.2 Redistribution capacity of RC sections: non-hinge region remains elastic

5.2.1 Unplated RC hinge

The redistribution capacity of RC members has often been considered difficult to determine.

Using the code approach, that is the neutral axis depth approach, which ignores the behaviour of the non-hinge region and hence assumes that it remains elastic as in Fig. 5(c), we need to determine the k_u factor, or the depth of the neutral axis in relation to the overall effective depth of the section, to ascertain the redistribution capacity of the section. In this example the k_u factor is 0.37, which can redistribute a maximum of 2.25% moment according to AS3600 (2001).

From the RBR approach, and whilst the non-hinge region remains elastic, Fig. 9 suggests that at failure there is a 65% moment redistribution capacity, much greater than according to AS3600. At yield, where the moment is 74.7 kNm and rotation 1.54E-3 radians, shown in Fig. 9 as the grey square, the redistribution capacity of the section is 4% which is much closer to that allowed in AS3600. This is expected as AS3600 does not consider strain hardening.

There is clearly a significant difference when comparing the moment redistribution allowed in AS3600 to that predicted at ultimate using RBR theory. The primary difference in the techniques is that the RBR approach considers the ductility of the reinforcing bars and the sliding capacity of the concrete, whilst the k_u approach only considers how under-reinforced the concrete section is without considering the material properties. As an example, the fracture strain of the reinforcing bars is not considered in the k_u approach, however it can clearly influence the ductility of the section and hence the redistribution capacity. Furthermore, the RBR approach is sensitive to material properties. As an example, consider reducing the fracture stress of the steel to 450 MPa, whilst maintaining the strain hardening modulus at 2,000 MPa. The reduced bar fracture stress reduces the ultimate moment capacity at bar fracture to 81.3 kNm, and the rotation at bar fracture to 4.4E-3 radians. According to these parameters, this section has a moment redistribution capacity of 11% at failure, which is much closer to that allowed under AS3600, and significantly less than the 65% for the previous material properties. This is just one example of the sensitivity of the RBR technique to material parameters which allows it to be used for a wide range of reinforcement.

5.2.2 Plated RC hinge

Consider increasing the applied static moment beyond 183kNm through moment redistribution from a plated section. We know from previous experience that externally bonded plates debond at low strains, minimising their ability to provide significant increases in flexural strength prior to debonding. If we wanted to provide a plated section with ductility, then NSM plates are required. NSM plates have greater bond transfer capacities, providing higher debonding forces and, therefore, greater increases in moment capacity. NSM plates also debond at larger slip values providing greater rotations at failure and, therefore, greater moment redistribution capacities. The NSM plating arrangement shown in Fig. 12 is analysed for moment redistribution, where we provide FRP with 20% the total cross sectional area of the reinforcing bars. This section is the same as the unplated RC section in Fig. 7, other than the addition of the NSM FRP plates, with properties as shown in Fig. 12.

The use of NSM plates provides a significantly greater increase in moment capacity at debonding failure, where from the RBR approach debonding failure commences at a moment of 128 kNm, a rotation of 6.4E-2 radians, and where the cracked flexural rigidity of the plated section is 7.1E+12 mm⁴. At the “*end of debonding*”, where debonding extends beyond the hinge region and where the progression of debonding is explained in detail in the companion paper (Haskett *et al.* 2010), the moment remains at 128 kNm, but the rotation increases to 1.5 E-1 radians.

Assuming a span depth ratio of 18, from Eq. (2) the moment redistribution capacity at the “*start of debonding*” is 57% and 76% at the “*end of debonding*”. In this example, at the “*start of*

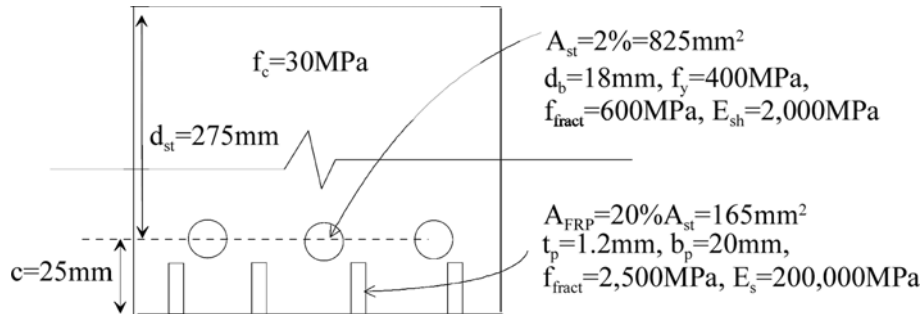


Fig. 12 NSM plated section

debonding”, with $M_{hog} = 128$ kNm and K_{MR} 57%, to allow full redistribution to occur the sagging region can be plated such that its moment is increased to 317 kNm. As before, to ensure that an additional rotation requirement is not induced in the hinge by the midspan rotation, the plating must be designed such that the section remains elastic up to a moment of 317 kNm. In this case this would allow the full 57% moment redistribution to occur.

6. Conclusions

It has been shown that the following three structural mechanics models are necessary to allow reinforced concrete beams to be designed for ductility and in particular moment redistribution: a moment-rotation-hinge model that quantifies the moment rotation capacities and which depends in particular on the reinforcement bond-slip characteristics; a moment-redistribution-capacity model for hinges which requires the moment-rotation capacity; and a beam-moment-redistribution model that requires the hinge moment redistribution capacities. These models are generic as they can be applied to any type of reinforced concrete with any type of reinforcement just as long as the bond-slip characteristics are known and, hence, can easily differentiate between EB and NSM adhesively bonded reinforcement as well as steel reinforcing bars. Hence, analysis tools are now available for specifically designing FRP plated beams not only for strength but also for ductility and for developing simpler design approaches.

Acknowledgements

The research was supported by an Australian Research Council Discovery Grant “Development of innovative fibre reinforced polymer plating techniques to retrofit existing reinforced concrete structures”.

References

- AS 3600-2001 (2001), Standards Australia.
- Concrete Society (2000), “Design guidance for strengthening concrete structures using fibre composite

- materials”, Technical Rep. No. 55, Crowthorne, Berkshire, U.K.
- Bencardino, F., Spadea, G. and Swamy, N. (2002), “Strength and ductility of reinforced concrete beams externally reinforced with carbon fiber fabric”, *ACI Struct. J.*, **99**, 163-171.
- Benlloch, J., Parra, C.J. and Valcuende, M. (2002), “Ductility of reinforced concrete beams strengthened with CFRP strips and fabric”, *ACI, Proceedings of the 6th International Symposium on FRP Reinforcement for Concrete Structures*, FRPRCS-6, 337-346.
- Duthinh, D. and Starnes, M. (2004), “Strength and ductility of concrete beams reinforced with carbon fiber-reinforced polymer plates and steel”, *J. Compos. Constr.*, **8**(1), 59-69.
- El-Refai, S.A., Ashour, A.F. and Garrity, S.W. (2003), “Sagging and hogging strengthening of continuous reinforced concrete beams using carbon fiber-reinforced polymer sheets”, *ACI Struct. J.*, **100**(4), 446-453.
- International Federation for Structural Concrete, *fib* Task Group 9.3 (2001), “Externally bonded FRP reinforcement for RC structures”, Technical Rep., Lausanne, Switzerland.
- Hashemi, S.H., Maghsoudi, A.A. and Rahgozar, R. (2008a), “Flexural ductility of reinforced HSC beams strengthened with CFRP sheets”, *Struct. Eng. Mech.*, **30**(4), 403-426.
- Hashemi, S.H., Maghsoudi, A.A. and Rahgozar, R. (2008b), “Flexural ductility of reinforced HSC beams strengthened with CFRP sheets”, *Struct. Eng. Mech.*, **30**(4), 403-426.
- Haskett, M.H., Oehlers, D.J., Mohamed Ali M.S. and Wu, C. (2010), “Analysis of moment redistribution in FRP plated RC beams”, *J. Compos. Constr.-ASCE*, **14**(4), 424-433.
- Haskett, M.H., Oehlers, D.J., Mohamed Ali, M.S. and Wu, C. (2009), “Rigid body moment-rotation mechanism for reinforced concrete beam hinges”, *Eng. Struct.*, **31**, 1032-1041.
- Howser, R., Laskar, A. and Mo, Y.L. (2010), “Seismic interaction of flexural ductility and shear capacity in reinforced concrete columns”, *Struct. Eng. Mech.*, **35**(5), 593-616.
- Liu, I.S.T., Oehlers, D.J. and Seracino, R. (2006), “Tests on the ductility of reinforced concrete beams retrofitted with FRP and steel near-surface mounted plates”, *J. Compos. Constr.*, **10**(2), 106-114.
- Mahini, S.S. and Ronagh, H.R. (2009), “Numerical modelling of FRP strengthened RC beam-column joints”, *Struct. Eng. Mech.*, **32**(5), 649-665.
- Mukhopadhyaya, P., Swamy, N. and Lynsdale, C. (1998), “Optimizing structural response of beams strengthened with GFRP plates”, *J. Compos. Constr.*, **2**(2), 87-95.
- Oehlers, D.J. and Seracino, R. (2004), *Design of FRP and Steel Plated RC Structures: Retrofitting Beams and Slabs for Strength, Stiffness and Ductility*, Elsevier, Oxford, U.K.
- Oehlers, D.J., Liu, I., Ju, G. and Seracino, R. (2004), “Moment redistribution in continuous plated RC beams. Part 1 Tests”, *Eng. Struct.*, **26**(14), 2197-2207.
- Oehlers, D.J., Haskett, M.H., Mohamed Ali, M.S. and Griffith, M.C. (2010), “Moment redistribution in reinforced concrete beams”, *Proc. ICE Struct. Build.*, **163**(3), 165-176.
- Panagiotakos, T.B. and Fardis, M.N. (2001), “Deformations of reinforced concrete members at yielding and ultimate”, *ACI Struct. J.*, **98**(2), 135-148.
- Sharma, A., Reddy, G.R., Eligehausen, R., Vaze, K.K., Ghosh, A.K. and Kushwaha, H.S. (2010), “Experiments on reinforced concrete beam-column joints under cyclic loads and evaluating their response by nonlinear static pushover analysis”, *Struct. Eng. Mech.*, **35**(1), 99-117.
- Yeh, F.Y. and Chang, K.C. (2007), “Confinement efficiency and size effect of FRP confined circular concrete columns”, *Struct. Eng. Mech.*, **26**(2), 127-150.